To the Graduate Council:

I am submitting herewith a thesis written by W. Grady Campbell entitled "The Decay of Mass-Separated ^{193}Pb to ^{193}Tl." I have examined the final copy of this thesis for form and content and recommend that it be accepted in partial fulfillment of the requirements for the degree of Master of Science, with a major in Physics.

Carrol R. Bingham
Carrol R. Bingham, Major Professor

We have read this thesis and recommend its acceptance:

Robert W. Lide

Leo P. Riedinger

Accepted for the Council:

C. W. Minkel
Vice Provost
and Dean of The Graduate School

STATEMENT OF PERMISSION TO USE

In presenting this thesis in partial fulfillment of the requirements for a Master's degree at the University of Tennessee, Knoxville, I agree that the Library shall make it available to borrowers under rules of the Library. Brief quotations from this thesis are allowable without special permission, provided that accurate acknowledgement of source is made.

Permission for extensive quotation from or reproduction of this thesis may be granted by my major professor, or in his absence, by the Head of Interlibrary Services when, in the opinion of either, the proposed use of the material is for scholarly purposes. Any copying or use of the material in this thesis for financial gain shall not be allowed without my written permission.

Signature Grady Campbell

Date June 6, 1985

THE DECAY OF MASS-SEPARATED ^{193}Pb TO ^{193}Tl

A Thesis

Presented for the

Master of Science

Degree

University of Tennessee, Knoxville

W. Grady Campbell

August 1985

ABSTRACT

Mass-separated samples of ^{193}Pb produced by W(^{16}O,xn) and Ta(^{20}Ne,pxn) reactions were collected by the UNISOR isotope separator operating on-line to the Oak Ridge Isochronous Cyclotron. N-type germanium radiation detectors and a Si(Li) radiation detector were used to gather multiscaled gamma-ray and conversion electron singles data and gamma-gamma and gamma-conversion electron coincidence data. A decay scheme was deduced from these data.

The decay rate of the $13/2^+$ isomer of ^{193}Pb was measured to be 5.65±0.07 minutes. Low spin states found in ^{193}Tl give evidence of a low-spin isomer of ^{193}Pb, but the half-life of 5.72±0.31 minutes found for it does not differ significantly from that of the high-spin isomer.

Shell-model states of $s_{1/2}$, $d_{3/2}$, and $h_{11/2}$ were observed and interpreted as proton hole states weakly coupled to a spherical ^{194}Pb core. Shell-model states of $h_{9/2}$ and $i_{13/2}$ were observed and interpreted as proton particle states strongly coupled to an oblate ^{192}Hg core. The expected state due to a proton hole coupled to a proton two particle-two hole state in a ^{194}Pb core was searched for but not observed.

The experimental results were compared to the triaxial-rotor-plus-particle model of Meyer-ter-Vehn. The experimentally discovered members of the $h_{9/2}$ structure were found to be in excellent agreement with those predicted by this rigid triaxial rotor model.

TABLE OF CONTENTS

CHAPTER		PAGE
I.	INTRODUCTION	1
	A. Previous Studies	1
	B. Goals	4
II.	EXPERIMENTAL	6
	A. Experimental Procedure	6
	B. Gamma-ray Singles Data	8
	C. Gamma-Gamma Coincidence Data and Decay Scheme	14
	D. Conversion Electron Data, Multipolarities of Transitions and Spin Assignments	26
III.	INTERPRETATION	39
IV.	CONCLUSION	47
	LIST OF REFERENCES	49
	VITA	52

LIST OF TABLES

TABLE PAGE

1. Gamma-ray energies and relative intensities in ^{193}Pb decay 12
2. Coincident gamma rays found in ^{193}Pb decay 15
3. Electron shell ratios and spin multipolarities in ^{193}Tl 31
4. Internal conversion coefficients and spin multipolarities in ^{193}Tl 33
5. Spin states in ^{193}Tl 36

LIST OF FIGURES

FIGURE		PAGE
1.	Decay Curves for the 392.4 keV transition in the decay of the high-spin isomer in ^{193}Pb	10
2.	Gamma Rays in ^{193}Pb decay	11
3.	Gamma rays coincident with the 365.5, 882.9 and 894.9 keV transitions in ^{193}Pb decay	18
4.	Gamma rays coincident with the 392.4, 323.8 and 431.1 keV transitions in ^{193}Pb decay	20
5.	Gamma rays coincident with the 636.9, 288.0 and 370.4 keV transitions in ^{193}Pb decay	22
6.	Gamma rays coincident with the 532.5 keV transition in ^{193}Pb decay and the decay scheme of levels associated with this transition	24
7.	Gamma rays coincident with the 943.5, 789.6 and 757.1 keV transitions in ^{193}Pb decay	25
8.	The portion of the ^{193}Pb decay scheme that includes the levels associated with the $s_{1/2}$ ground state	27
9.	The portion of the ^{193}Pb decay scheme that includes the levels associated with the $h_{9/2}$ isomeric state	28
10.	Conversion electrons in ^{193}Pb decay	30
11.	Single-particle states in odd-mass Tl nuclei for masses 191 to 199	41
12.	Levels in neutron-deficient Tl nuclei due to an $h_{9/2}$ proton coupled to a Hg core	44

CHAPTER I

INTRODUCTION

A. Previous Studies

Levels in ^{193}Tl were first studied by Diamond, et al.[1] along with a range of odd and even masses of thallium nuclei. They observed a 365.5 keV transition having a multipolarity of 71%E2+(29±10)%M1 and identified it as a $3/2^+$ to $1/2^+$ transition. From systematics they postulated a $9/2^-$ level lying less than 25 keV above the $3/2^+$ state, and measured the half-life of the $9/2^-$ state as 2.11 minutes. They had expected the $h_{9/2}$ state to lie much higher, above the shell gap and thought the $9/2^-$ level to be produced by coupling an $h_{11/2}$ proton hole to 2 unpaired neutrons or neutron holes.

Members of this group did a later study[2] of levels in light odd-mass thallium nuclei. They decided the $9/2^-$ level was in fact a low-lying or intruder $h_{9/2}$ orbital and found several members of a rotational band based on this state. This intruder state was explained by oblate deformation and a gain in pairing energy when the odd proton is excited up to the next shell. Also discovered was an $i_{13/2}$ orbital state. They found 24 transitions, placing 17 in a decay scheme and made confident assignments of 7 spins.

The initial in a series of experiments at UNISOR to study the decay of ^{193}Pb[3] placed 11 lines in a decay scheme also having 7 spin assignments. An attempt was made to find the energy of the E3 transition that depopulates the $9/2^-$ level by looking for L x-rays

corresponding to electrons being ejected from the thallium atom by the highly converted low-energy transition. Vacancies from the L shell were found to be fewer than 20% of the 365.5 keV gamma-ray transitions; therefore, the transition must occur by M conversion or above. This put an upper limit of 13 keV on the transition energy.

Kahler[4] describes an in-beam study of levels in ^{193}Tl in which 31 transitions were found and 21 of these placed in a decay scheme of 17 levels of up to spin 23/2, with spin determination being made by angular distribution measurements. The rotational bands built by $h_{9/2}$ and $i_{13/2}$ protons coupled to an oblate core were seen to spin 19/2 and 21/2 respectively.

A ^{193}Pb decay study at UNISOR conducted by Collins, et al.[5] found 31 transitions and placed 30 of them in a decay scheme having 21 levels. For the first time, low spin states other than the $3/2^+$ state and an $h_{11/2}$ structure were seen. The half-lives of the $3/2^-$ ground state and the $13/2^+$ isomeric state of ^{193}Pb were measured as 4.0±0.7 minutes and 5.57±0.12 minutes, respectively. Conversion electron data collection was attempted but source intensities were too low.

The intrusion of states from above the shell gap has been discussed[2] and collinear atomic beam laser spectroscopy has given further experimental support to the part played by deformation in lowering these intruder levels.[6] An interesting feature of the $h_{9/2}$ structure was the even spacing of the yrast rotational band, characteristic of strong coupling, and the lack of variation of this structure with changing neutron number and changing deformation; at

the same time, the energy of the $9/2^-$ level relative to ground state was seen to vary with neutron number and deformation. This was explained by the laser spectroscopy work; neutron pairing correlations act to counter the effect of changing deformation on the rotational moment of inertia of the different odd mass Tl nuclei.

Theoretical work relevant to transitional odd-mass nuclei and encompassing the species under study here has been done by Meyer-ter-Vehn[7,8], who made calculations based on particles and holes coupled to triaxial rotating cores. In the Meyer-ter-Vehn model, the Davydov[9] approximation to the collective motion of an even-even core and the quasiparticle moving within its field is expressed as a function of the deformation, asymmetry and the Fermi surface energy of the core. The first two parameters may be approximated from the lowest excited states of the adjacent even nuclei and the last from the Nilsson level scheme, but noting the adjustment required to exactly reproduce experimental observation can give insight into the nature of the nuclei under study.

Fairly extensive Meyer-ter-Vehn calculations have been collected by Riedinger, et al.[10] for the states associated with the $h_{9/2}$ proton state in ^{193,195,197}Tl. The Riedinger paper compared the calculations to the experimental data of Collins, et al.[5] and found good agreement for a rigidly asymmetric triaxial core. A higher value for the deformation factor than predicted from the Hg core was required to fit the experimental results. Two levels were found which were quite sensitive to the asymmetry factor γ, the first $5/2^-$ and the second $13/2^-$. For ^{193}Pb decay, the best agreement between predicted

energies and branching ratios occurred for $\gamma=40^{o}$, implying that degree of oblateness to the ^{193}Tl nucleus. The Fermi surface energy had to be set to 0.22 in order to bring a K=7/2 band down sufficiently to explain a second $9/2^{-}$ and third $13/2^{-}$, but a more physical explanation was thought to include the effect of higher shell states, likely the $f_{7/2}$, mixing with the $h_{9/2}$ state which is assumed pure by the model, thus lowering the K=7/2 band.

Recently there has been excitement about low-lying 0^{+} states in even-mass $^{192-198}$Pb due to a proton two particle-two hole (2p-2h) configuration;[11] levels in neutron-deficient Tl due to proton holes coupling to this 0_2^{+} Pb core state should exist. It is thought they have been found in odd masses 187-191, and it is predicted by extrapolation that the first such state, a $3/2_2^{+}$ level, should lie about 690 keV above the $3/2^{+}$ level that is the first excited state in ^{193}Tl.[12]

B. Goals

Neutron-deficient Tl nuclei make interesting subjects in the study of nuclear shapes. Adjacent nuclei have different shapes; the slightly oblate deformation of Hg gives way with increasing atomic number to spherical shapes in Pb, and the particle and hole couplings that result should be characteristic of the shapes of different cores. Not only are two shapes expected to be in evidence; as many as four coexisting shapes have been observed in odd-mass nuclei in the area of light-mass Tl due to couplings with 0^{+} and 0_2^{+} states of neighboring core nuclei. The proposed explanation of such states may be tested by finding whether the odd proton blocks the postulated

proton pair states in a Hg core, pushing them to higher energy, or the states are unaffected, which would indicate that some other effect is at work. The coupling to a deformed Pb core should be visible, even if the coupling to a deformed Hg core is not expected to be seen.

It is intended that this work augment the decay scheme established by the studies mentioned above. The spin states of levels heretofore assigned theoretically or from systematics may be confirmed or refuted by the first gamma-conversion electron data available for this isotope, the collection of which was made possible by source development work at UNISOR. The conversion electron data should also make likely the identification of the E0 transitions in ^{193}Tl that correspond to the newly found 0_2^+ to 0^+ ground state transition and the transitions between the structure built on these levels in ^{194}Pb. Lastly, the energy levels and intensities will be examined in light of the Meyer-ter-Vehn model.

CHAPTER II

EXPERIMENTAL

A. Experimental Procedure

The experimental data were collected at the Holifield Heavy Ion Research Facility at Oak Ridge National Laboratory. The Oak Ridge Isochronous Cyclotron was used as a source of energetic heavy ions to impact a refractory metal target with a subsequent fusion-neutron evaporation reaction. This target formed part of the ion source of the UNISOR mass separator, which was used to provide beams of reaction products selected by mass. These beams were directed onto mylar tapes and thus samples of the products could be collected, withdrawn from the beamline and examined.

Two experiments are analyzed in this thesis. In the first of these, a beam of 141.5 MeV $^{16}O^{5+}$ from the cyclotron struck a 2.0 mg/cm^2 natural tungsten target. The recoil nuclei deposited upon and diffused through a graphite felt-tungsten carbide catcher into the separator ion source with a 5% Xe-95% He support gas used to increase the speed of release of the products from the catcher to the source. A target of ^{182}W was tried for one source change of this run to increase the yield of ^{191}Pb that was being collected simultaneously but the switch proved unhelpful.

Samples were formed by collecting a mass-separated ion beam on aluminized mylar tapes; these were transported out of the beamline into a counting chamber where their activity was detected by 10%

Ge(Li) and N-type Germanium detectors placed 180^{o} from each other. Under computer control, a freshly exposed section of tape was moved in front of the detectors and data were taken for 12 consecutive 30 second intervals with counts during each of these intervals being stored by the computer as a separate spectrum or plane. This cycle was repeated and the decay of the peaks as shown by these spectra would determine the lifetime of each isomer and aid in identifying to which isomer each peak belonged. The energy and intensity of each peak may be found with better statistics by summing these different spectra. At the same time as this gamma multiscaled singles data were being taken gamma-gamma-time coincidence list data were being recorded and stored by the computer for later analysis. The aim of this analysis is to find coincident transitiitions and construct a decay scheme.

During the second experimental run, the cyclotron beam was 129.5 MeV $^{20}Ne^{5+}$, the target was a 1.1 mg/cm^{2} tantalum window, the catcher was hafnium carbide on graphite felt and the support gas was again 5% Xe-95% He. Employed this time were a 15% N-type germanium and a Si(Li) detector. The computer was programmed for multiscaled data of 10 planes of 60 seconds each and gamma-electron-time coincidence list data were taken. The aim of this experiment was to deduce multipolarities of transitions by examining ratios of electron and gamma-ray intensities and comparing these ratios to theoretical conversion coefficients.

B. Gamma-ray Singles Data

All data analysis was done on the Perkin-Elmer computer systems at the Holifield Heavy Ion Research Facility. The first step was to find the intensities of all the peaks in each of the planes of the gamma multiscale data. This was accomplished by the computer program TIZZY, which automatically finds and fits peaks, outputting their intensity computed by two methods, a simple sum and a computation of the area under the gaussian fitted peak. By calculating the lifetime of each peak one may determine which are of interest. The only impurity of any consequence was ^{193}Tl, produced by electon capture and beta emission by the ^{193}Pb nucleus; the strongest transition seen in its decay had an intensity of 4.0% of the 365.5 keV transition intensity in ^{193}Pb decay.

The 392.4 keV peak is known from earlier work[2] to be the highest intensity transition to populate the $9/2^-$ level and its decay rate should be that of the of the $13/2^+$ isomeric state of ^{193}Pb. The multiscale data for this transition were least squares fitted to a logarithmic curve and a half-life of 5.65±0.07 minutes was determined. This is in good agreement with the half-life found by Collins, et al.[5] The 365.5 keV transition is the highest intensity transition to be fed from the ground state of ^{193}Pb but it is also fed by the isomeric level in ^{193}Tl. The transition that populates the 365.5 keV level, that of 404.8 keV, was chosen to determine the half-life of the ^{193}Pb ground state utilizing the same technique as above; a half-life of 5.72±0.31 minutes was the result. The 882.9 keV transition in coincidence with

the 404.8 keV transition was used to check the half-life of the ground state; the value according to this second transition was 5.71±0.44 minutes. The value of 5.72±0.31 minutes found here is not in agreement with 4.0±0.7 minutes found by Collins, et al.[5], but the disagreement is not far outside the limit imposed by the errors.

Figure 1 is a plot of the experimental points and the computed curves for the decay of the 392.4 and 404.8 keV transitions. The 404.8 keV transition was not seen in every plane of the multiscale data. The experimental data points for the 335.1 keV transition of ^{193}Tl decay are included in the figure as representative of the decay rate of that daughter of ^{193}Pb in this experiment. The decay rate for the 335.1 keV transition is not simple; the intensity of the transition grows as Pb decays to Tl and wanes as Tl decays to Hg. Included in the figure is the decay seen for the 323.8 keV transition that is found in both ^{193}Pb and ^{193}Tl decay. The two components of this decay were calculated as described below and also appear in Figure 1.

All the planes were summed and the resulting spectrum was examined utilizing the computer program SPASM, a program using graphics monitors to interactively find and fit peaks and compute peak areas. The summed gamma-ray singles spectrum collected by the N-type detector may be seen in Figure 2. The detector energy calibration and efficiency as a function of energy was determined using a mixed standard source prepared by The Radiochemical Centre[13]. The transition energy and intensity of all peaks determined to occur in ^{193}Pb decay are found in Table 1.

The 323.8 keV line required special attention; in addition to

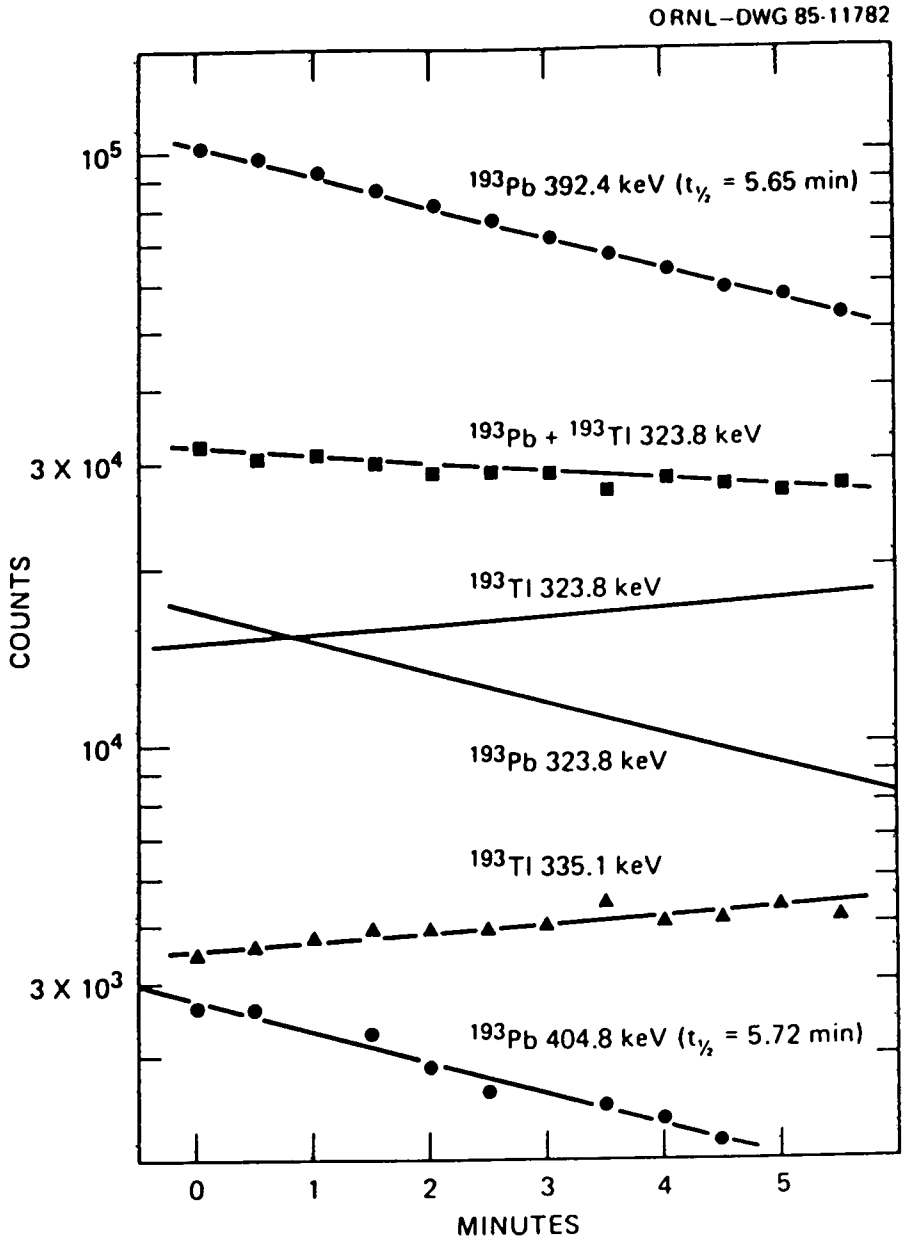


Figure 1. Decay curve for the 392.4 keV transition in the decay of the high-spin isomer in ^{193}Pb. Decay curves for the 323.8 keV transition that occurs in both ^{193}Pb and ^{193}Tl decay, the 335.1 keV transition in ^{193}Tl decay and the 404.8 keV transition in the decay of the low-spin isomer in ^{193}Pb are also shown.

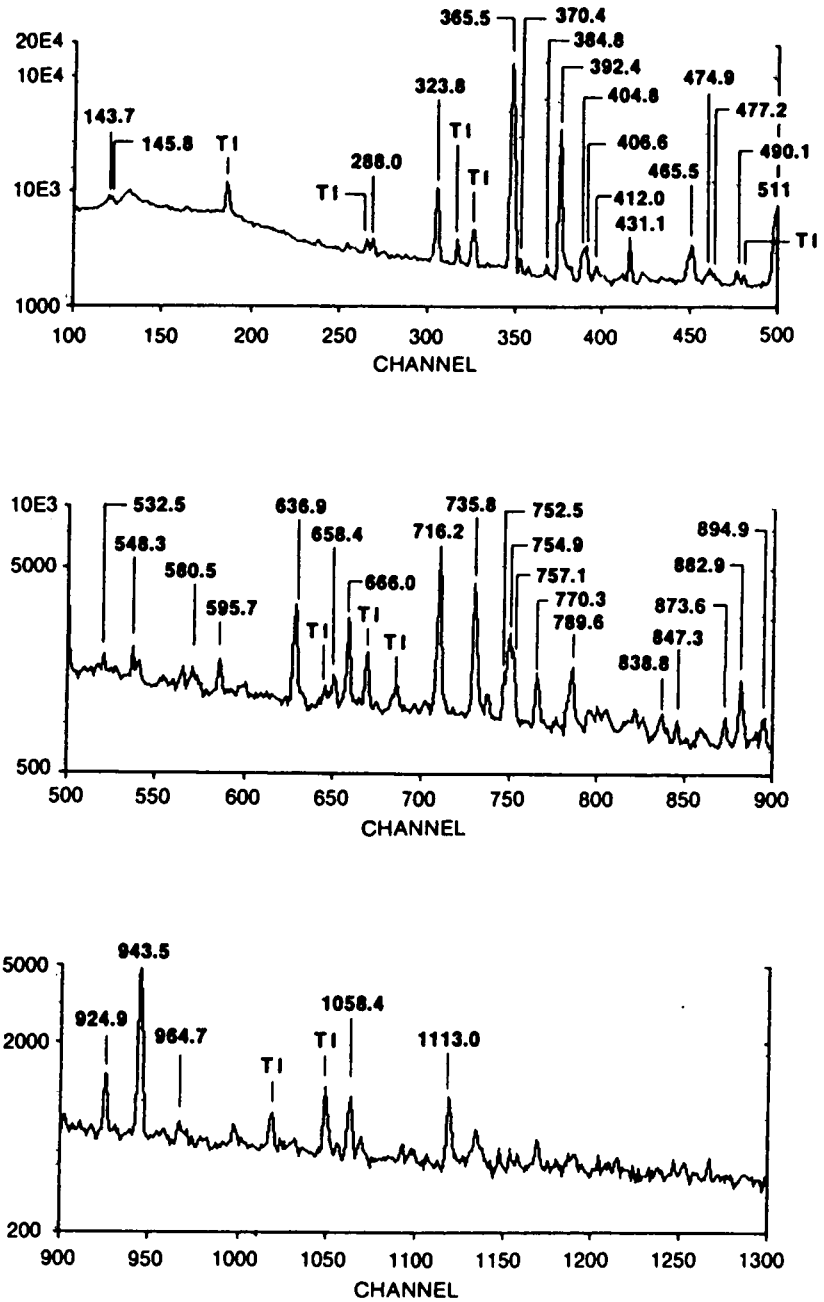


Figure 2. Gamma rays in ^{193}Pb decay. Peaks are labelled with their energies in keV. There are impurity peaks from the decay of ^{193}Tl.

Table 1. Gamma-ray energies and relative intensities in ^{193}Pb decay.

Gamma-ray Energy (keV)	Relative Intensity
143.7 ±0.1	0.56 ±0.02
145.8 ±0.1	0.43 ±0.01
288.0 ±0.1	0.62 ±0.01
321.4 ±0.2	0.58 ±0.07
323.8 ±0.2	2.63 ±0.11
365.5 ±0.1	100 ±1.7
370.4 ±0.2	0.39 ±0.10
384.8 ±0.1	0.22 ±0.01
392.4 ±0.1	20.75 ±0.27
404.8 ±0.1	0.76 ±0.04
406.6 ±0.1	1.03 ±0.04
412.0 ±0.1	0.36 ±0.02
416.2 ±0.1	0.12 ±0.02
431.1 ±0.1	1.28 ±0.02
465.5 ±0.1	1.24 ±0.06
474.9 ±0.1	0.47 ±0.02
477.2 ±0.1	0.24 ±0.01
490.1 ±0.1	0.42 ±0.01
532.5 ±0.2[a]	0.24 ±0.01
548.3 ±0.1	0.44 ±0.01
580.5 ±0.2	0.29 ±0.02
595.7 ±0.1	0.51 ±0.02
636.9 ±0.1	2.43 ±0.09

Table 1. (continued)

Gamma-ray Energy (keV)	Relative Intensity
658.4 ±0.1	0.40 ±0.02
666.0 ±0.1	2.07 ±0.06
716.2 ±0.2	6.14 ±0.19
735.8 ±0.1[a]	3.91 ±.14
752.5 ±0.1	0.90 ±0.07
754.9 ±0.1	1.75 ±0.08
757.1 ±0.1	1.17 ±0.07
770.3 ±0.1	0.86 ±0.06
789.6 ±0.1	0.98 ±0.05
838.8 ±0.1	0.28 ±0.02
847.3 ±0.1	0.27 ±0.02
873.6 ±0.1	0.37 ±0.02
882.9 ±0.1	1.03 ±0.05
894.9 ±0.2	0.37 ±0.02
924.9 ±0.1	1.43 ±0.08
943.5 ±0.1	8.31 ±0.48
964.7 ±0.1	0.31 ±0.02
1058.4 ±0.2	1.30 ±0.08
1113.0 ±0.1	1.74 ±0.11
1596.2 ±0.1	0.56 ±0.01

[a]Doublet in ^{193}Pb decay. The components are elsewhere resolved using coincidence techniques.

being a substantial peak in ^{193}Pb decay it is the largest peak in ^{193}Tl decay. A standard Pb decay rate was established by the 392.4 keV transition multiscale data and similarly for Tl by the 335.1 keV transition. It was then possible to determine the contributions to the 323.8 keV line due to each of these isotopes by making a least squares fit of the decay data with a linear combination of the standard decay rate curves (see Figure 1). The contribution to the summed spectrum by Pb decay was determined to be 39.2% and the total intensity found by the computer was reduced accordingly and entered into Table 1.

C. Gamma-Gamma Coincidence Data and Decay Scheme

Using the computer, it is possible to form a two-dimensional matrix of coincident events where the two axes represent the two channel numbers or energies that were recorded by each detector for that event. To be classified as a coincident event, the two detector signals must occur within a set time window, on the order of 30 nanoseconds wide. By looking down the rows or across the columns of the matrix one can see graphically what transition energies are in coincidence and by careful study one can deduce the pattern of energies given off in the de-excitation of the nucleus. Table 2 is a summary of coincident events found in ^{193}Pb decay.

The 365.5 keV transition is the largest intensity transition found in the gamma-ray singles data. The spectra of gamma rays in coincidence with the 365.5, 882.9 and 894.9 keV gamma rays are shown in Figure 3. The 404.8, 873.6, 882.9 and 894.9 keV transitions are seen in coincidence with the 365.5 keV transition. The 873.6 keV

Table 2. Coincident gamma rays found in ^{193}Pb decay.

Gamma-ray Energy (keV)	Energy of Gamma rays in Coincidence[a] (keV)
143.7	392.4(s), 735.8(m)
145.8	392.4(s), 735.8(m)
288.0	370.4(m), 636.9(s)
321.4	392.4(w), 431.1(w)
323.8	392.4(s), 412.2(w), 431.1(m), 465.5(m), 474.9(w) 752.5(w)
365.5	404.8(s), 873.6(w), 882.9(s), 894.9(w)
370.4	288.0(m), 384.8(w), 392.4(m), 532.5(w), 636.9(m) 924.9(m)
384.8	370.4(w), 636.9(w), 924.9(w)
392.4	143.7(w), 145.8(w), 323.8(s), 370.4(w), 406.6(m) 416.2(w), 431.1(m), 465.5(m), 474.9(w), 477.2(w) 532.5(w), 548.3(w), 580.7(w), 666.0(s), 735.8(s) 752.5(w), 755.4(m), 838.8(w), 848.4(w), 964.7(w) 1113.0(m), 1596.2(w)
404.8	365.5(s), 873.6(m)
406.6	392.4(s), 735.8(s)
412.0	323.8(w), 392.4(w)
416.2	392.4(w)
431.1	321.4(w), 323.8(s), 392.4(s), 416.2(w), 716.2(s)
465.5	323.8(s), 392.4(s), 406.6(m), 465.5(w), 666.0(m) 735.8(s), 755.4(w), 1113.0(m)
474.9	323.8(m), 392.4(w)
477.2	392.4(s)
490.1	636.9(s)
532.5[b]	288.0(w), 370.4(m), 392.4(s), 532.5(w), 636.9(w) 658.4(w), 924.9(m)

Table 2. (continued)

Gamma-ray Energy (keV)	Energy of Gamma rays in Coincidence[a] (keV)
548.3	392.4(s), 666.0(s), 1058.4(m)
580.5	288.0(w), 532.5(w), 636.9(w), 924.9(m)
595.7	392.4(m)
636.9	288.0(s), 370.4(w), 384.8(w), 490.1(m), 580.5 658.4(m)
658.4	636.9(s)
666.0	392.4(s), 548.3(m)
716.2	406.6(w), 412.2(m), 416.2(w), 431.1(s), 752.5(m) 838.8(w), 847.3(w)
735.8[b]	143.7(w), 145.8(w), 392.4(s), 406.6(m), 465.5(m) 943.5(w)
752.5	323.8(m), 392.4(s), 716.2(s)
754.9	321.4(w), 392.4(s), 416.2(w)
757.1	943.5(s)
770.3	873.6(w)
789.6	943.5(s)
838.8	323.8(w), 392.4(s), 716.2(m)
847.3	323.8(m), 392.4(m), 716.2(m)
873.6	365.5(m), 404.8(m), 770.3(m)
882.9	365.5(s), 894.9(w)
894.9	365.5(s), 882.9(m)
924.9	370.4(s), 532.5(m), 580.5(m)
943.5	735.8(m), 757.1(s), 789.6(m)
964.7	392.4(s)

Table 2. (continued)

Gamma-ray Energy (keV)	Energy of Gamma rays in Coincidence[a] (keV)
1058.4	548.3(m)
1113.0	392.4(s)
1596.2	392.4(s)

[a]An s denotes strong coincidence, an m denotes medium or probable coincidence and a w denotes weak or possible coincidence.

[b]Doublet placed twice in decay scheme.

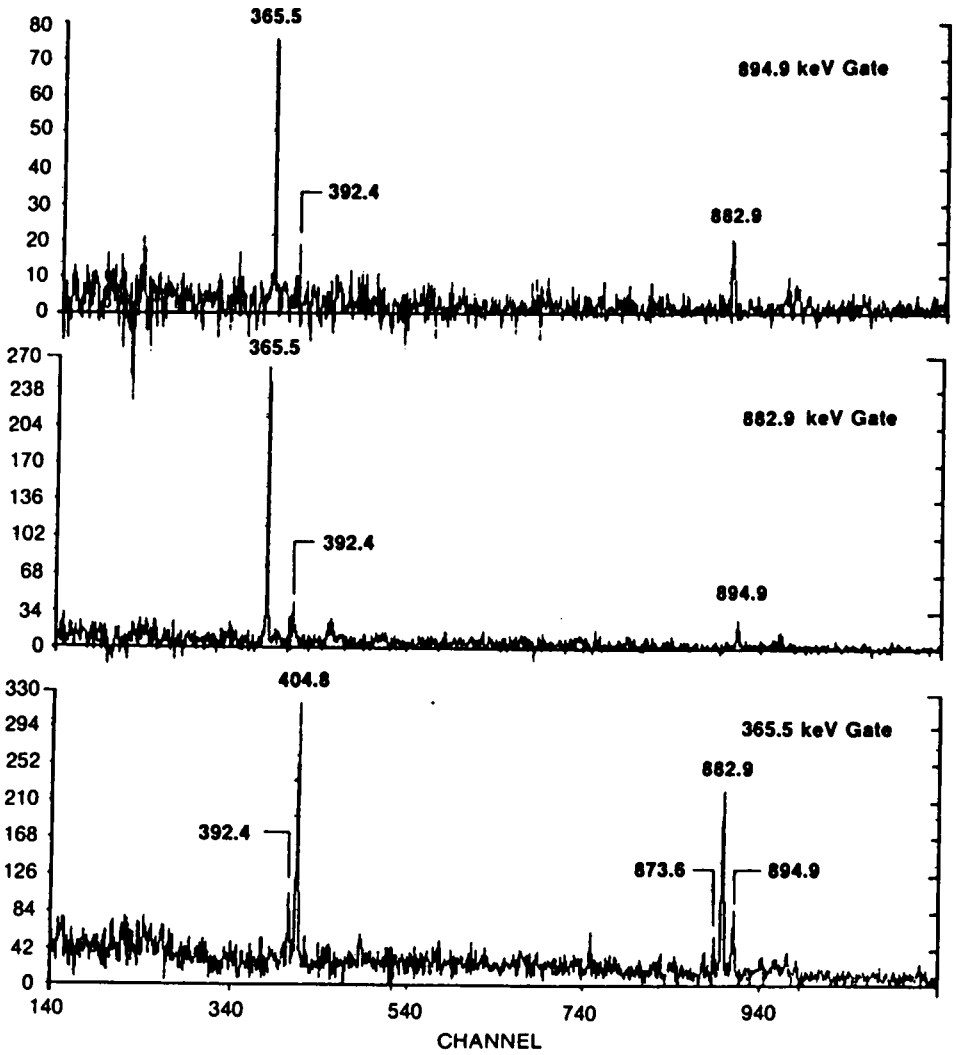


Figure 3. Gamma rays coincident with the 365.5, 882.9 and 894.9 keV transitions in ^{193}Pb decay. Peaks are labelled with their energies in keV.

transition was also seen to be coincident with the 404.8 keV transition and was placed so as to form a cascade built of 365.5, 404.8 and 873.6 keV transitions. Because it is a correct sum and it is seen to be coincident with the 873.6 keV line, the 770.3 keV transition was placed parallel to the 365.5 and 404.4 keV transitions. In consideration of its higher intensity, the 882.9 keV line was placed beneath the coincident 894.9 keV line.

All the above transitions originate from levels whose relationships to the 365.5 keV transition are easily seen. Previous studies place this structure of levels on the $1/2^+$ ground state. The transitions that remain all populate the $9/2^-$ isomeric state whose transition to the 365.5 keV level is of such small energy it has not been determined in previous studies and was not seen in this experiment.

The largest intensity transition found in the total coincidence spectrum, which is a count of all coincident events at each energy, is the 392.4 keV transition. Among the transitions coincident with it are those of 323.8 keV and 431.1 keV; the spectra of gamma rays coincident with these three are shown in Figure 4. These three transitions were placed in a cascade and crossover transitions of 716.2 and 754.9 keV were found by taking sums and examining coincidence data. Transitions of 321.4 and 416.2 keV were found to be separately in coincidence with this cascade. They are paralleled by crossover transitions of 752.5 and 838.6 keV, respectively, leading to the level depopulated by the 323.8 and 716.2 keV transitions. In a similar manner the 412.0 keV line was placed atop the 323.8 keV line and its

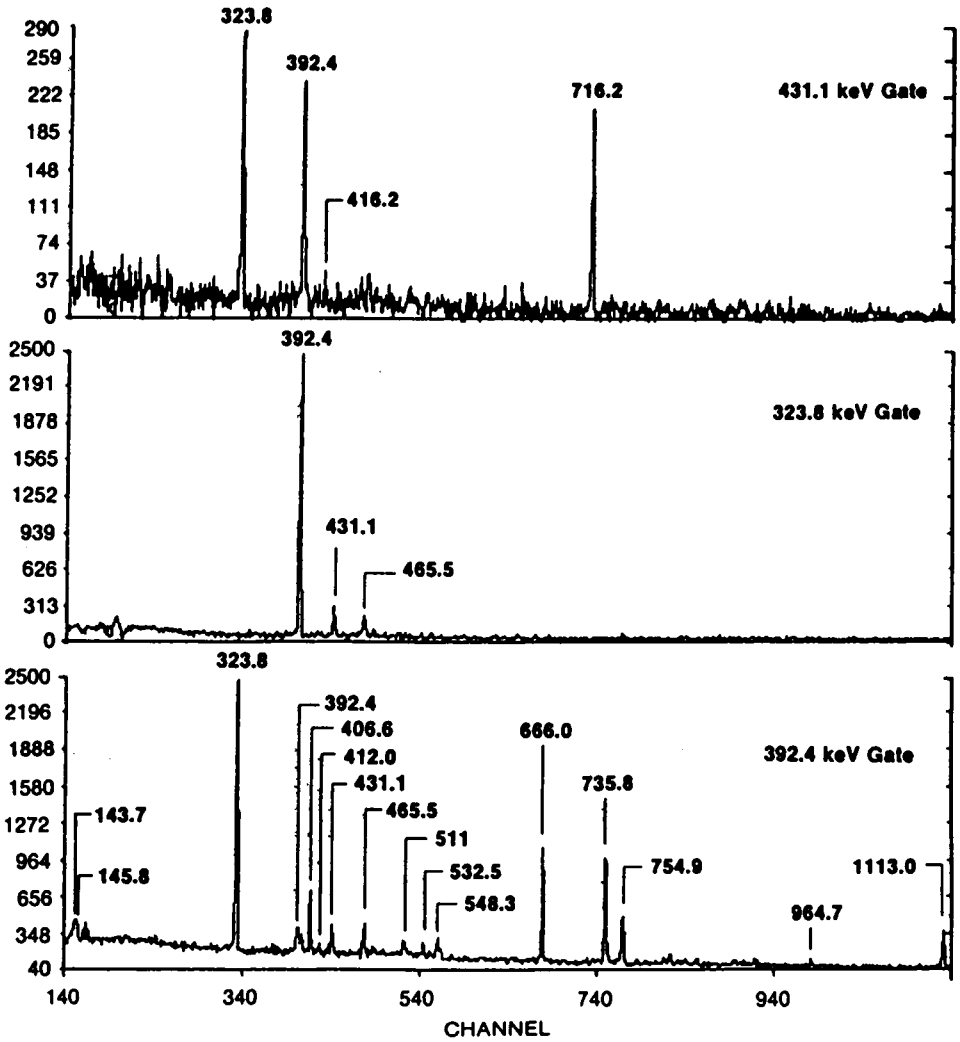


Figure 4. Gamma rays coincident with the 392.4, 323.8 and 431.1 keV transitions in ^{193}Pb decay. Peaks are labelled with their energies in keV.

crossover determined to be via a 735.8 keV transition. Four transitions were found to be coincident only with the transition of 392.4 keV and originate on levels that are not depopulated by another transition; these are the 477.2, 595.7, 964.7 and 1596.2 keV transitions. Similarly, there are 2 transitions that depopulate levels not depopulated by another transition above the 323.8 keV transition; these are the 474.9 and 838.8 keV transitions. The level depopulated by the 412.0 keV transition is fed by 4 transitions that necessitated additional levels, the 143.7, 145.8, 406.6, and 465.5 keV transitions.

Another large but not entirely separate family of transitions feed the isomeric level; these have as their lowest transition one of 636.9 keV. There is a cascade of 636.9, 288.0 and 370.4 keV; the spectra of gamma rays coincident with each of these transitions are shown in Figure 5. The appearance of the 392.4 and 323.8 keV transitions in these spectra is explicable only as accidental coincidences between some of the highest intensity lines in the coincidence spectrum and are not confirmed by the coincidence spectra of 392.4 and 323.8 keV. The crossovers here are 924.9 and 658.4 keV. There are a transition of 490.1 keV (coincident solely with the 636.9 keV line) and of 532.5 and 384.8 keV (coincident solely with the cascade of 636.9, 288.0 and 370.4 keV lines) that depopulate levels that are not depopulated by another transition.

There are two transitions that tie the groups of transitions mentioned in the previous two paragraphs together. The first of these is the 580.5 keV transition that is found in coincidence with the 636.9 and 288.0 keV cascade; the level that it depopulates is also

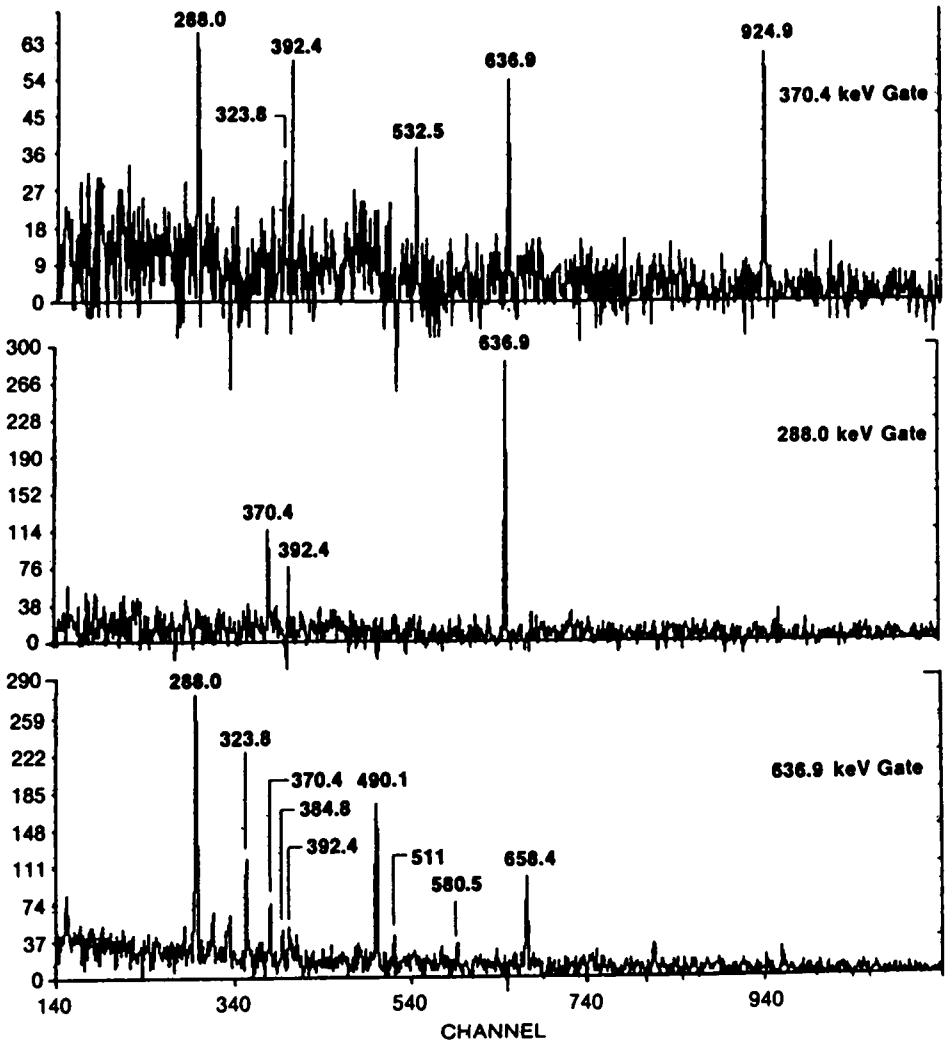


Figure 5. Gamma rays coincident with the 636.9, 288.0 and 370.4 keV transitions in ^{193}Pb decay. Peaks are labelled with their energies in keV.

depopulated to the first level above the isomeric level by a transition of 1113.0 keV. No transition could be seen that is in coincidence with both the 580.5 and the 1113.0 keV transition. The second, the 532.5 keV transition, was difficult to place with certainty and its coincidence spectrum and the decay scheme containing it may be seen in Figure 6. It is clearly in coincidence with the 392.4 keV transition and it fits neatly into the gap between the levels above the 392.4 keV line and the 288.0 keV line; thus it should be found atop the 392.4 keV transition. It is also clearly in coincidence with the 636.9, 288.0 and 370.4 keV cascade and also itself, establishing it as a doublet with its second component placed at the top of the cascade. The intensity of each component was determined by taking the intensity shown in the 658.4 keV coincidence spectrum, showing only the upper component, adjusting the result according to the strength of that transition and subtracting from the total to get the intensity of the lower component of the doublet.

There is a 1058.4 keV transition seen only in coincidence with a 548.3 keV transition. In coincidence with the 548.3 keV transition is a 666.0 keV transition that by summing and coincidence considerations may be placed to form a cascade with the 392.4 keV transition in parallel with the 1058.4 keV transition.

One final set of transitions remains to be discussed. It is made up of the 943.5 keV transition and the three transitions that were found to lie atop it, of 735.8, 757.1 and 789.6 keV. The spectra of coincident gamma rays for several of these transitions are seen in Figure 7. The 735.8 keV transition is a doublet. It was easily fitted

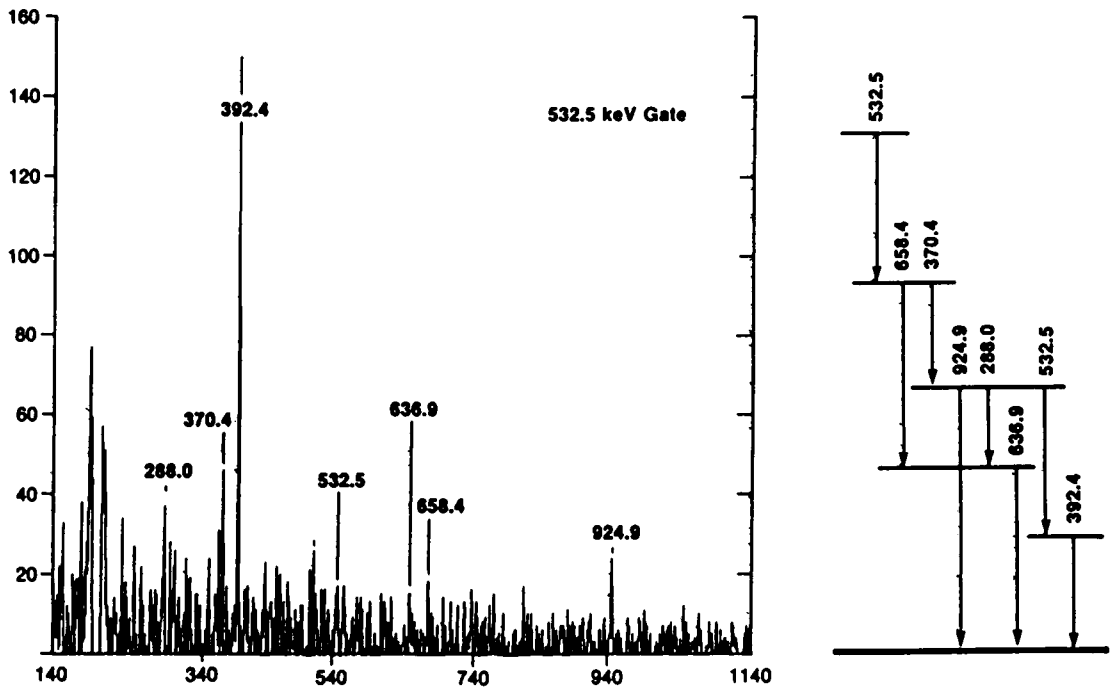


Figure 6. Gamma rays coincident with the 532.5 keV transition in ^{193}Pb decay and the decay scheme of levels associated with this transition. Peaks are labelled with their energies in keV.

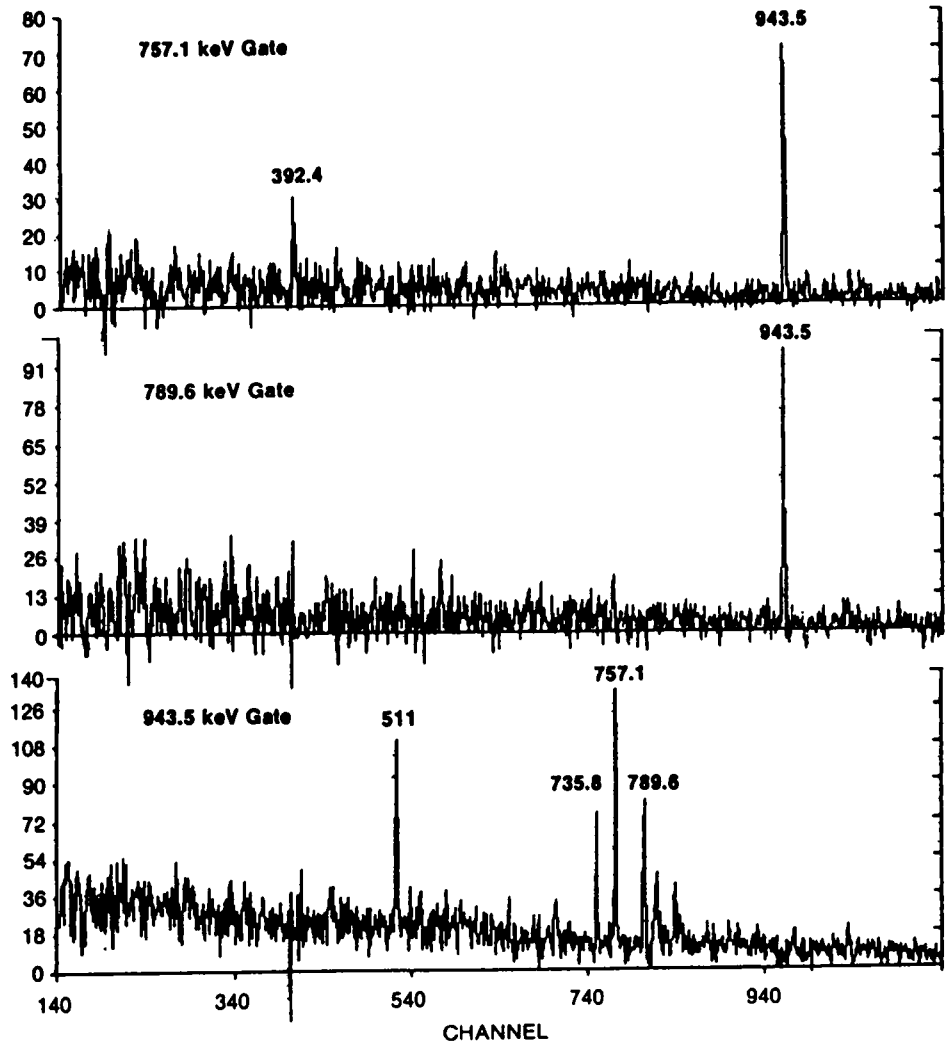


Figure 7. Gamma rays coincident with the 943.5, 789.6 and 757.1 keV transitions in ^{193}Pb decay. Peaks are labelled with their energies in keV.

into the decay scheme as a transition that led to the level depopulated by the 392.4 keV transition and it was further discovered to have a mutual coincidence relationship with the 943.5 keV transition. No transitions between these levels and the levels already placed were found.

Figure 8 is the decay scheme constructed of transitions that directly feed the $1/2^+$ ground state. Also shown is the unobserved transition that depopulates the $9/2^-$ isomeric state. Figure 9 is the decay scheme constructed of transitions that directly feed that isomeric state. The levels in the latter decay scheme are not precisely known, but the energy of the E3 transition, denoted in the figure as δ, is less than 13 keV.[3]

D. Conversion Electron Data, Multipolarities of Transitions and Spin Assignments

During de-excitation a nucleus has energy carried away by energetic gamma rays, by atomic electrons or, for energy level changes greater than 1.02 MeV, by electron-positron pairs. These processes compete with each other; pair production, when allowed, occurs typically every 10^3 or 10^4 gamma-ray emissions and conversion electron emission occurs with a probability governed by the electromagnetic multipolarity of the transition. Thus, the ratio of the number of energetic electrons emitted from the nuclear atom to the number of gamma rays emitted by the nucleus in a transition between energy levels is a signature of the multipolarity of the transition. Such ratios are called internal conversion coefficients and aside from

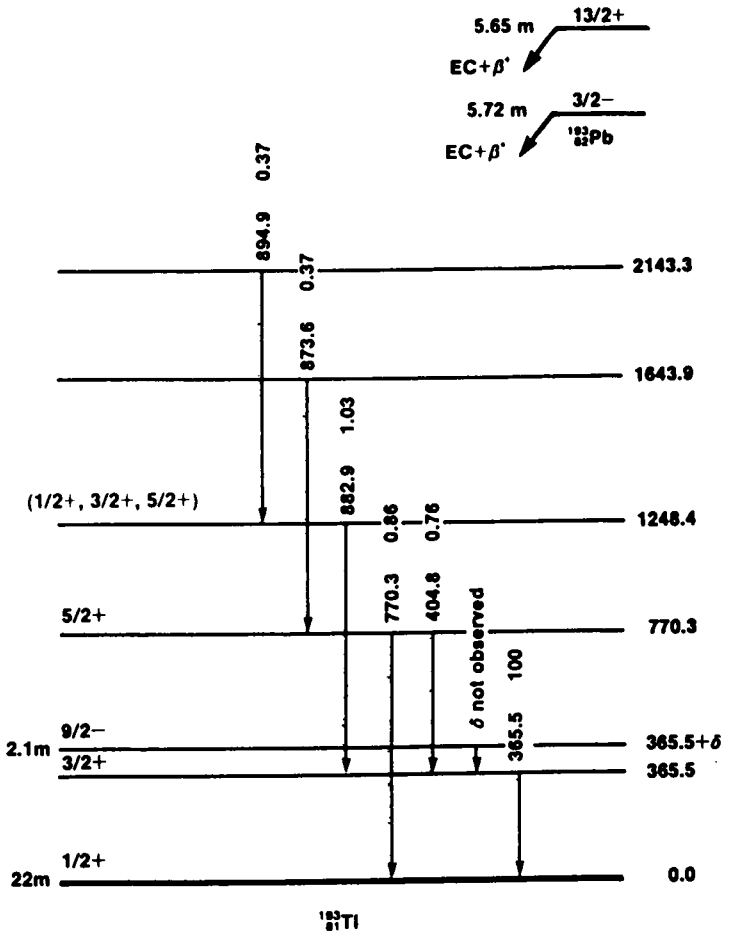


Figure 8. The portion of the ^{193}Pb decay scheme that includes the levels associated with the $s_{1/2}$ ground state. The energy in keV and intensity are given for each transition.

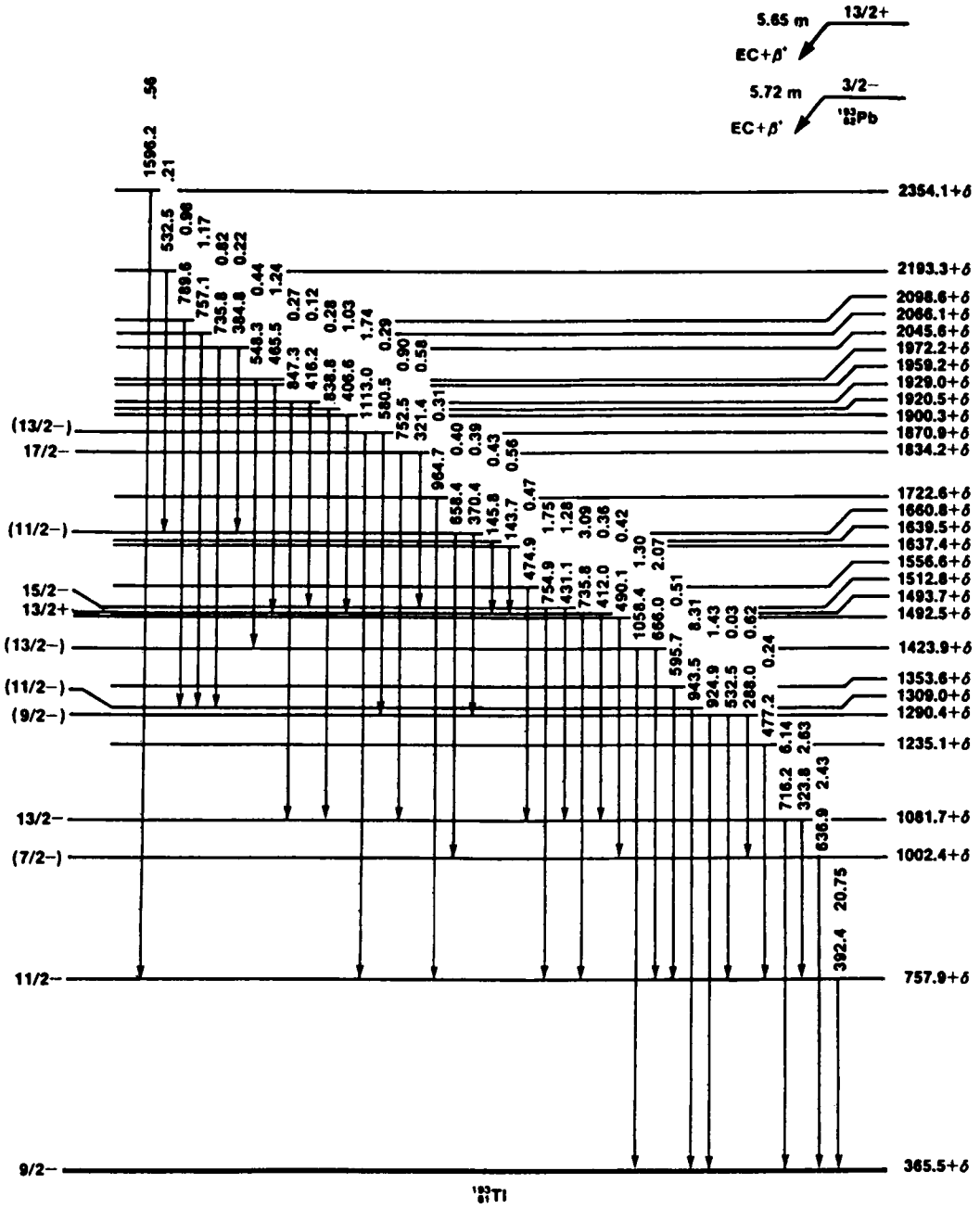


Figure 9. The portion of the ^{193}Pb decay scheme that includes the levels associated with the $h_{9/2}$ isomeric state. The energy in keV and intensity are given for each transition.

transition multipolarity and energy depend only on atomic number. For transitions that have several allowed multipolarities, the degree to which each occurs is indicated by the weighting of the coefficients of each competing multipolarity. In addition, the ratios of electrons emitted from each subshell can identify the transition multipolarity.

Tables of internal conversion coefficients are readily available; the one used in this study covers atomic numbers 30 through 104 and is by Rosel, et al.[14] Cubic spline interpolation is an excellent way to approximate much physical data and the most accurate method of obtaining intermediate values from these tables; the interpolating curves have continuous second derivatives at the tabular points for a very smoothed fit to the theoretical data points. This was the method used for interpolating the tables.

The conversion electron spectrum obtained by the Si(Li) detector is shown in Figure 10. Conversion electrons from ^{193}Tl decay were again the only significant contaminant.

A mixed antimony-europium standard source[15] was used in the calibration of the N-type detector. Unfortunately, an accurate calibration of the electron detector was not obtained. For the energy range encountered in this experiment, it was deemed safe to assume a constant efficiency for the electron detector. Its absolute efficiency had to be established by examining the ratio of the K shell intensity to the summed intensity of the unresolved L_I and L_{II} subshells for the 365.5 and 392.4 keV transitions and determining their multipolarity. This required no knowledge of absolute detector efficiency. The results for these and other subshell ratios are given in Table 3. The

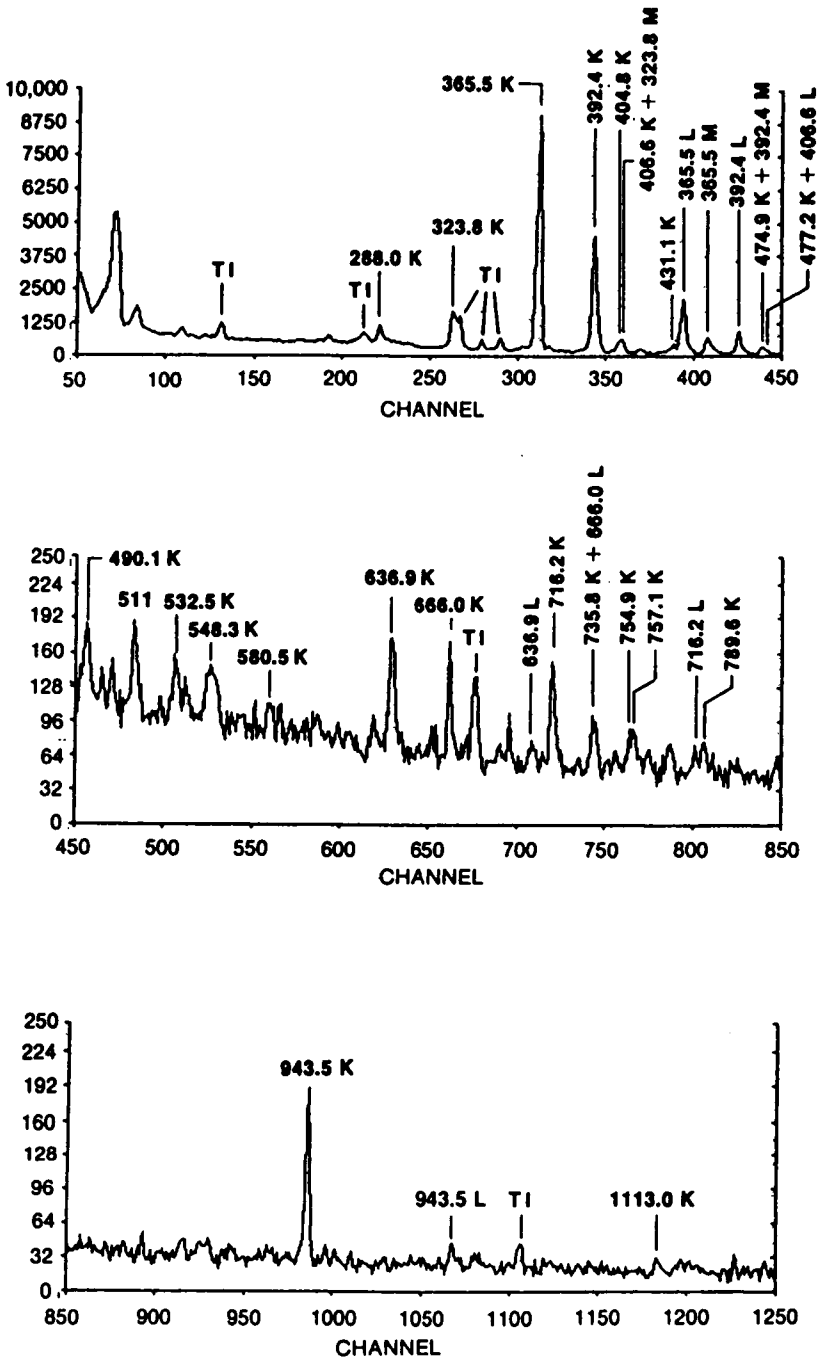


Figure 10. Conversion electrons in ^{193}Pb decay. Peaks are labelled with the energy in keV of the transition and the electron shell. There are impurity peaks from the decay of ^{193}Tl.

Table 3. Electron shell ratios and spin multipolarities in ^{193}Tl.

Energy (keV)	Electron Shell	Experimental Ratio	Theoretical Ratio E1	E2	M1	Assigned Multipolarity
365.5	$K/(L_I+L_{II})$	3.97 ±.12	6.72	2.96	5.94	E2+(33.9±4.0)%M1
	K/M	15.3 ±.92	28.8	8.47	25.6	E2+(39.9±5.4)%M1
392.4	$K/(L_I+L_{II})$	5.85 ±.16	6.72	3.16	6.00	M1+(5.3±5.3)%E2
636.9	$K/(L_I+L_{II})$	4.54 ±.68	6.84	4.51	6.09	E2
716.2	$K/(L_I+L_{II})$	5.03 ±1.30	6.88	4.81	6.03	E2

experimental internal conversion coefficients were then normalized such that they best fit the multipolarities given by these two subshell ratios. The end result had a discrepancy of 13.8% between the multipolarities predicted by subshell ratios and gamma-conversion electron ratios for the 365.5 and 392.4 keV transitions. A thorough search for doublets at 392.4 and 365.5 keV was conducted without success. The Si(Li) detector was checked for efficiency variations and found flat from 428.2 to 645.5 keV using known $^{194}Tl^{16}$ peaks that contaminated the spectrum when the wrong mass was selected for a short time. The experimental internal conversion coefficient of the 645.5 keV peak produced again the normalization defined as above. The amount of ^{194}Tl data was too small to give good statistics but it did confirm the results found earlier. The experimental and theoretical internal conversion coefficients and the multipolarities assigned by them are given in Table 4.

The low energy transitions of 143.7 and 145.8 keV were unresolved in the electron spectrum and no multipolarity could be assigned them. The electron spectrum at the 288.0 keV gamma-ray transition was contaminated by the 284.9 keV transition K electron of ^{193}Tl decay and its experimental conversion coefficient was high as a result. The peaks at 406.6, 474.9 and 477.2 keV all contained contributions from L and M subshell electrons of lower energy transitions and the experimental conversion coefficients were at least double that of a theoretical M1 transition. The 532.5 keV transition had a large error in the corresponding electron peak intensity, probably because it is an unresolved doublet. These seven transitions

Table 4. Internal conversion coefficients and spin multipolarities in ^{193}Tl.

Gamma-ray Energy (keV)	Experimental Conversion Coefficient	Theoretical Conversion Coefficient E1	E2	M1	Assigned Multipolarity
321.4	0.25 ±0.04	0.0202	0.0547	0.282	M1+(13.8±33.1)%E2
323.8	0.29 ±0.02	0.0199	0.0538	0.278	M1
365.5	0.075 ±0.001	0.0155	0.0410	0.209	E2+(20.1±0.8)%M1
370.4	0.20 ±0.12	0.0150	0.0397	0.202	M1
392.4	0.18 ±0.01	0.0132	0.0348	0.173	M1
404.8	0.096 ±0.03	0.0123	0.0324	0.159	M1+(50.3±25.3)%E2
431.1	0.20 ±0.03	0.0107	0.0281	0.132	M1
465.5	0.042 ±0.006	0.00893	0.0237	0.104	E2+(22.5±7.0)%M1
490.1	0.14 ±0.04	0.00792	0.0210	0.0882	M1
548.3	0.11 ±0.04	0.00615	0.0164	0.0622	M1
580.5	0.048 ±0.007	0.00546	0.0145	0.0531	M1+(14.3±19.0)%E2
636.9	0.036 ±0.003	0.00462	0.0121	0.0434	M1+(25.1±8.0)%E2
666.0	0.030 ±0.003	0.00430	0.0112	0.0402	M1+(36.7±10.9)%E2
716.2	0.012 ±0.001	0.00381	0.00983	0.0354	E2+(8.0±4.4)%M1

Table 4. (continued)

Gamma-ray Energy (keV)	Experimental Conversion Coefficient	Theoretical Conversion Coefficient E1	E2	M1	Assigned Multipolarity
735.8[a]	0.0076 ±0.0013	0.00364	0.00935	0.0336	E1, E2+M1
752.5	0.013 ±0.0043	0.00351	0.00897	0.0321	E2+(17.4±18.4)%M1
754.9	0.012 ±0.003	0.00348	0.00891	0.0318	E2+(14.0±14.2)%M1
757.1	0.017 ±0.004	0.00347	0.00886	0.0317	E2+(34.0±20.9)%M1
770.3	0.0073 ±0.0030	0.00337	0.00858	0.0305	E2
789.6	0.019 ±0.003	0.00321	0.00817	0.0288	E2+(50.0±13.7)%M1
882.9	0.015 ±0.003	0.00260	0.00657	0.0216	M1+(41.1±22.8)%E2
924.9	0.0081 ±0.0019	0.00238	0.00599	0.0188	E2+(16.7±16.6)%M1
943.5	0.013 ±0.001	0.00228	0.00576	0.0176	M1+(37.8±4.6)%E2
964.7	0.0063 ±0.0029	0.00218	0.00551	0.0164	E2+(7.4±26.1)%M1
1113.0	0.0066 ±0.0017	0.00163	0.00413	0.00994	E2+(43.0±28.9)%M1

[a]The doublet at 735.8 keV has one component that appears to be an E1 transition from systematics and theoretical considerations further discussed in the text. An exact calculation of the other component has not been attempted due to the presence of 666.0 keV transition L electrons in this peak.

were omitted from the table. The 735.8 keV conversion coefficient has multiple contributions to error and appears to be between E1 and E2 in multipolarity; it is mixed with the 666.0 keV transition L line and it is a doublet. The assignment of E1 to the lower component forming a level at 1493.7+δ appears reasonable from systematics considerations. Unfortunately the other transition depopulating this level, 412.0 keV, cannot be seen in the electron spectrum and cannot confirm this assignment. The other component would then be a mix of E2 and M1 multipolarity with exact proportions made indeterminate by the 666.0 keV transition L electron contribution. Many other transitions could not be included in Table 4 because their electron peak could not be seen and above roughly 700 keV the background noise made it impossible to assign an upper limit to electron intensity that could discriminate an E1 from an M1/E2 mixture for any but the larger intensity transitions.

All multipolarities assigned were either E1, E2, M1, or a mixture of E2 and M1. Of these, an E1 indicates a parity change and the rest indicate no parity change between levels. For an odd number of nucleons, where the levels are of half-integer spin, an E1 or M1 transition can change spin magnitude by at most one and an E2 by at most two units. The levels for which a spin was determined appear in Table 5 along with a list of possible spin assignments according to experimentally determined internal conversion coefficients.

An extensive search was conducted to find transitions having E0 components that would populate the $3/2^+$ level as a result of a second $3/2^+$ level as discussed in the previous chapter. Also searched

Table 5. Spin States in ^{193}Tl.

Level Energy (keV)	Assigned Spin
0.0	$1/2^+$
365.5	$3/2^+$
365.5+δ	$9/2^-$
757.9+δ	$11/2^-$
770.3	$5/2^+$
1002.4+δ	$7/2^-$, $9/2^-$, $11/2^-$
1081.7+δ	$13/2^-$
1248.4	$1/2^+$, $3/2^+$, $5/2^+$
1290.4+δ	$7/2^-$, $9/2^-$, $11/2^-$
1309.0+δ	$7/2^-$, $9/2^-$, $11/2^-$
1423.9+δ	$9/2^-$, $11/2^-$, $13/2^-$
1492.5+δ	$5/2^-$, $7/2^-$, $9/2^-$, $11/2^-$, $13/2^-$
1493.7+δ	$13/2^+$
1512.8+δ	$15/2^-$
1660.8+δ	$7/2^-$, $9/2^-$, $11/2^-$, $13/2^-$
1722.6+δ	$7/2^-$, $9/2^-$, $11/2^-$, $13/2^-$, $15/2^-$
1834.2+δ	$17/2^-$
1870.9+δ	$9/2^-$, $11/2^-$, $13/2^-$
1959.2+δ	$11/2^+$, $13/2^+$, $15/2^+$
1972.2+δ	$7/2^-$, $9/2^-$, $11/2^-$, $13/2^-$, $15/2^-$
2045.6+δ	$5/2^-$, $7/2^-$, $9/2^-$, $11/2^-$, $13/2^-$
2066.1+δ	$5/2^-$, $7/2^-$, $9/2^-$, $11/2^-$, $13/2^-$
2098.6+δ	$5/2^-$, $7/2^-$, $9/2^-$, $11/2^-$, $13/2^-$

for to prove nonexistence was a partially E0 transition that would populate the $9/2^-$ level as a result of a second $9/2^-$ level. The sign of a transition having an E0 component is a large ratio of conversion electrons to gamma rays for that transition; i.e., a large internal conversion coefficient. A number of techniques may be used to find such a transition. The gamma-conversion electron coincidence spectra may be examined for a large number of electrons in coincidence with a gamma-ray transition. The electron spectrum in coincidence with the 365.5 keV transition that depopulates the $3/2^+$ level was examined and there were no peaks that would be unexpected by the already established decay scheme. No transition would be expected to be coincident with the $9/2^-$ to $9/2_2^-$ transition. The multiscaled singles electron data were searched for transitions decaying with the proper lifetime, 5.65 minutes, to indicate that they belong in the ^{193}Pb decay. To get better statistics, three planes were summed to make three spectra of 3 minutes collection time each out of the original ten spectra of 1 minute each. Even with this summing, the statistics were still too poor to make determinations as to which isotope a transition belonged for any but the highest intensity transitions. The most likely method to succeed in exposing a large E0 strength in a transition appeared to be an examination of all conversion electron peaks that differed in energy from peaks in the gamma-ray spectrum by exactly the 85.5 keV predicted by the atomic K shell binding energy for transitions in a Tl nucleus. No candidates for transitions having an E0 component in ^{193}Tl were discovered. It is possible that the E0 transition is a doublet with some other transition but the

electron coincidence spectrum is weak enough to make resolving the transition in such a case unlikely.

CHAPTER III

INTERPRETATION

Odd-mass Pb of mass 199 up have as their ground state a $5/2^-$ state. Mass 197 marks the point at which the $3/2^-$ state falls below the $5/2^-$ state to become the ground state, which is the case for ^{193}Pb. An isomeric state of $13/2^+$ also exists, and it is predominantly the decay of this state that populates levels in ^{193}Tl. By mass 193, the $13/2^+$ state might very well lie below the $5/2^-$ state, requiring an unlikely E5 isomeric transition rather than the M4/M1 cascade to ground state seen in ^{197}Pb. However, the amount of low-spin activity is sufficiently large to indicate the existence of both states and that the lower state is populated via an isomeric transition rather than solely via the heavy ion fusion reaction. Unfortunately, the amount of activity is small enough that the transition could not be identified and the measured decay rate is questionable. A possible growth-decay combination in the decay of low-spin states could not be seen due to the low quality of the data. Thus, the decay rate of 5.72 minutes measured for the ground state of ^{193}Pb is due to the isomeric transition from the $13/2^+$ state, whose decay rate is more confidently taken to be 5.65 minutes and the ground state half-life is comparatively short, or else the transition occurs either not at all or to only a small extent and the two half-lives are approximately the same.

There are two isomeric levels in ^{193}Tl, the ground state has spin $1/2^+$ and the high-spin isomeric state has spin $9/2^-$. There are

few lines associated with the ground state, built on the $s_{1/2}$, $d_{3/2}$ and with less confidence, $d_{5/2}$ states, but the isomeric state has many lines occurring in the structures built on several states, the $h_{9/2}$, $h_{11/2}$ and $i_{13/2}$ states. Figure 11 shows these single-particle states in ^{193}Tl and includes odd masses 191-199 for comparison.

The low-spin levels of 365.5 and 770.3 keV have been assigned spins of $3/2^+$ and $5/2^+$, respectively, as a result of experimental internal conversion coefficients of the transitions between these levels. The 1248.4 keV level was found to be of spin 1/2, 3/2 or 5/2 with positive parity. The Meyer-ter-Vehn calculation in Riedinger, et al.[10] predicted a $5/2^-$ level to decay to either the $9/2^-$ or the $1/2^+$ level and it was thought the 1248.4 keV level might be that level in ^{193}Tl. The results of this study rule out the 1248.4 keV level as the predicted state, and no level was found to replace it as a candidate for the $5/2^-$ state.

Positive parity states of spin 1/2, 3/2 and 5/2 in ^{193}Tl are expected due to $s_{1/2}$, $d_{3/2}$ and $d_{5/2}$ proton holes coupled to a ^{194}Pb core. The $s_{1/2}$ and $d_{3/2}$ states are at the 0.0 and 365.5 keV levels. A level of 770.3 keV is somewhat low for a $d_{5/2}$ proton hole state and is about right for an $s_{1/2}$ proton hole coupled to the first excited state in ^{194}Pb, a 2^+ state at 964.2 keV.[17] A better candidate for the $d_{5/2}$ proton hole state is at the 1643.9 keV level, in analogy with the Collins[18] data for ^{195,197}Pb where $5/2^+$ levels were assigned at about this energy. Collins' data did not rule out a $3/2^+$ assignment for these levels and in this work no assignment of the 1643.9 keV level

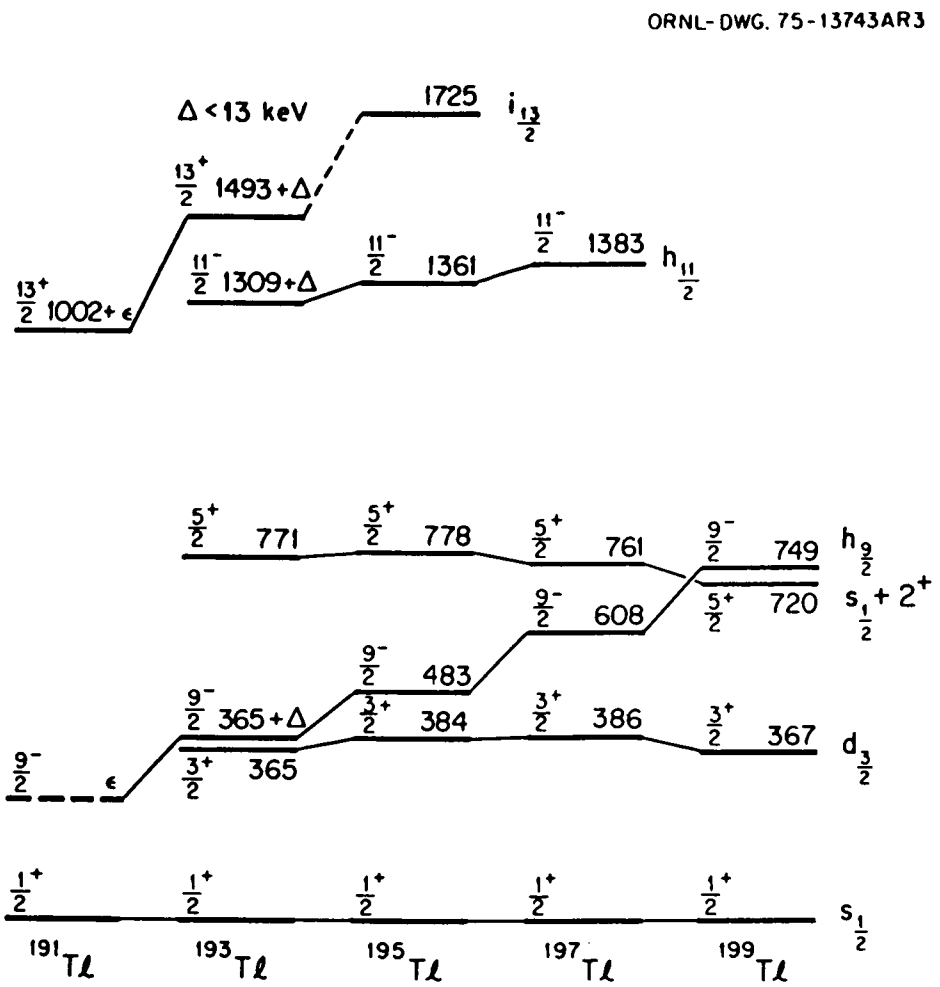


Figure 11. Single-particle states in odd-mass Tl nuclei for masses 191 to 199.

could be made, so it is but speculation that the $d_{5/2}$ proton hole state occupies this level.

The other proton hole state observed was due to an $h_{11/2}$ proton hole state coupled to a ^{194}Pb core. It was seen as a negative parity, spin 11/2 state decaying to the isomeric level and having a structure independent of other identifiable states. It could be exactly identified only by analogy to $^{195,197}Pb$ decay schemes as the M1/E2 mixed multipolarity of the 943.5 keV transition that depopulates this state made spin assignment ambiguous. The structure built on this state was apparently a multiplet structure due to coupling of the hole state to the 2^+ one phonon vibration of the core; such a structure would be expected to give seven levels of spin $7/2^-$ through $15/2^-$ grouped about 964 keV above the $11/2^-$ level. Only three lines of this multiplet could be identified and they were about 200 keV low; exact spin assignment for these multiplet levels that decay by E2/M1 transitions was impossible. Collins[18] identified more lines in this proposed multiplet in $^{195,197}Tl$; they also were lower in energy than expected. These levels also might be due to $s_{1/2}$ and $d_{3/2}$ states coupling to the 5^- and 7^- states that lie at 1820 and 2240 keV in ^{194}Pb.[17]

It can be seen from Figure 11 that all the states lying below the Z=82 shell gap, the proton hole states $s_{1/2}$, $d_{3/2}$, $h_{11/2}$ and possibly the $d_{5/2}$, which is not pictured, change little in energy from mass to mass in Tl isotopes. The vibrational type coupling seen for these states is indicative of weak coupling. The states lying above

the shell gap, the proton particle $h_{9/2}$ and $i_{13/2}$ states, trend downward in energy with decreasing neutron number.

The strongly coupled rotational band built on the $h_{9/2}$ level is well established to spin 17/2 by experimental conversion coefficients. There is a great deal of non-yrast structure associated with the $h_{9/2}$ state and it can best be examined in terms of the Meyer-ter-Vehn model introduced in the first chapter. The predictions of the model, discussed below, along with experimentally obtained results for ^{193,195,197}Pb are shown in Figure 12. Other than for the yrast rotational band, unambiguous spin assignments could not be made from experimental conversion coefficients, although in no case did the possible spin assignments contradict the predicted values. The K=7/2 and K=13/2 side bands are seen to spin 13/2 and 15/2 respectively. The K=5/2 side band is not seen in ^{193}Tl.

A comparison of the experimentally discovered structure built on the $h_{9/2}$ state with the triaxial-rotor-plus-particle model of Meyer-ter-Vehn showed excellent agreement for a deformation factor of -0.158, an asymmetry factor of 40^{o} and a Fermi surface energy of 0.22, in calculations originally reported by Riedinger, et al.[10] The deformation factor was raised somewhat from the theoretical value to reproduce the experimental levels. The final value is indicative of intermediate coupling, and the rotational band level spacing shows some shift due to Coriolis mixing, but due to oblate deformation of the Hg core, the level arrangement is that of the strong-coupling case. The asymmetry factor required adjustment to fit the energy level found for the second $13/2^{-}$ level, providing a means to postulate a

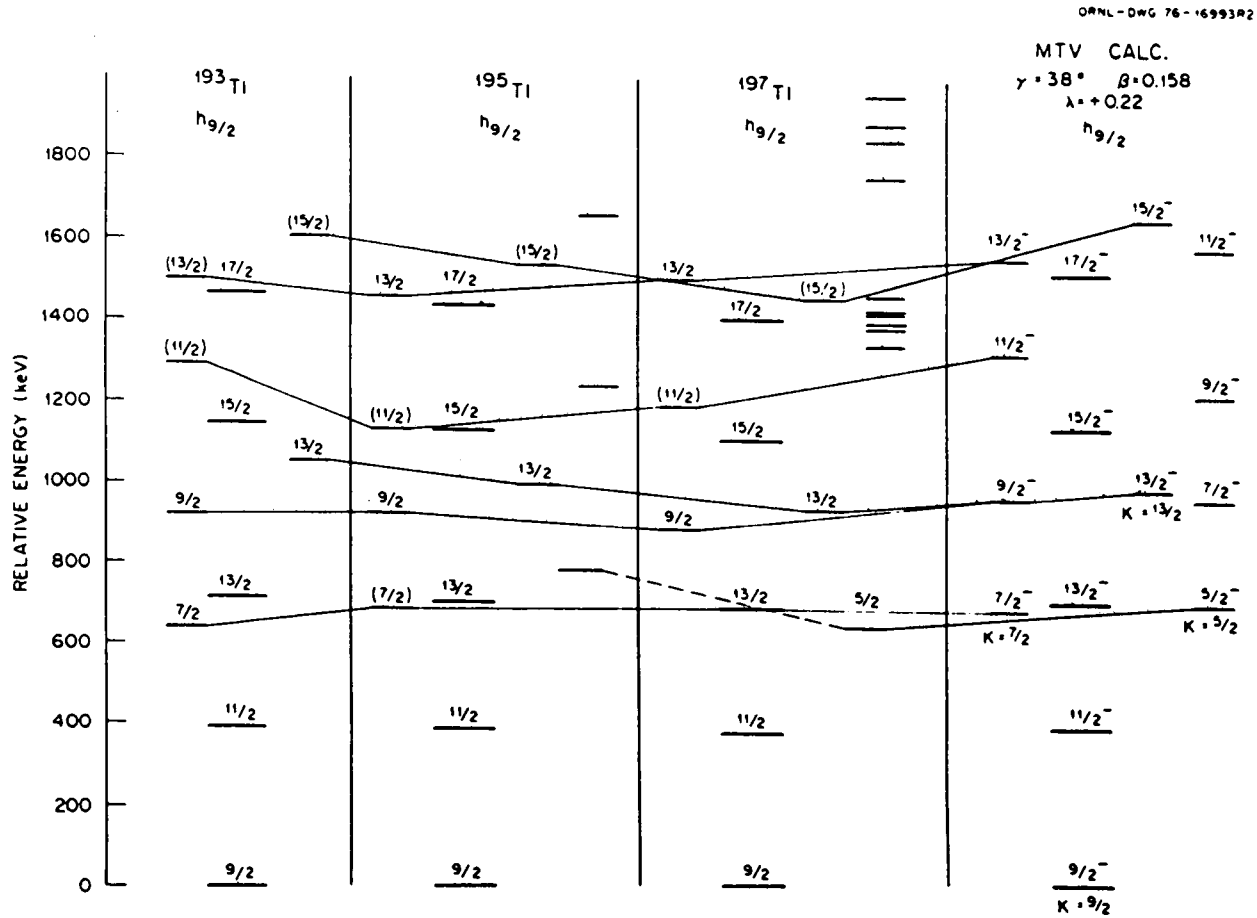


Figure 12. Levels in neutron-deficient Tl nuclei due to an $h_{9/2}$ proton coupled to a Hg core. Levels found experimentally for masses 193, 195 and 197 are compared to theoretical values.

precise shape for the ^{192}Hg nucleus. Other levels were not found to be as dependent on the exact asymmetry factor. The K=7/2 sideband predicted by the model was seen in its entirety for the first time in ^{193}Tl; as in ^{195,197}Tl, the Fermi surface is necessarily increased from the theoretical value to create theoretical levels to account for this sideband.

The $i_{13/2}$ state joins the $h_{9/2}$ state intruding below the shell gap, at 1128 keV higher. It shows itself as a positive parity, spin 13/2 level with its spin confirmed by experimental conversion coefficient data. There are no clear analogues to this level in higher odd masses of Tl, but they could be expected to occur at energies increasing in a similar manner to that of the $h_{9/2}$ state. Four levels feed this state, but only the 465.5 keV transition has a possible spin assigned. It depopulates a level known only to be $11/2^+$, $13/2^+$ or $15/2^+$. Lack of more complete knowledge of the structure built on this level prevents comment on the nature of this proton particle state, although it should be similar to the $h_{9/2}$ proton particle state. It is curious that such low-lying levels are found in the structure.

A proton particle state due to an $f_{7/2}$ orbital proton and a ^{192}Hg core might be expected to intrude somewhere in energy between the $h_{9/2}$ and $i_{13/2}$ single-particle states. Such a state would be a negative parity, spin 7/2 state; a candidate for this state is the level lying at 1002.4+δ. That level has already been attributed to the $h_{9/2}$ structure, but it could only be theoretically produced by adjusting theoretical parameters, though the adjustment was seen to be justified. The proposed single-particle state would trend in energy

with the other proton states identified in odd-mass Tl isotopes (see Figure 11), and the structure built on it should be characteristic of strong coupling to an oblate core.

CHAPTER IV

CONCLUSION

The $13/2^+$ isomer of ^{193}Pb was found to have a half-life of 5.65±0.07 minutes. The $3/2^-$ ground-state of ^{193}Pb had a half-life that could not be differentiated from that of the isomeric state; it was found to have a half-life of 5.72±0.31 minutes. There was sufficient low-spin activity in ^{193}Tl to indicate the existence of the ground state in ^{193}Pb, but this could not be supported or contradicted by the decay data.

The adjacent nuclei of Hg and Pb were taken as cores giving rise to shell-model states. Expected proton hole states in $s_{1/2}$, $d_{3/2}$, $d_{5/2}$ and $h_{11/2}$ orbitals were in evidence, as were states attributed to the $s_{1/2}$ and $h_{11/2}$ states coupling to the first phonon vibration of the Hg core. The $d_{5/2}$ state was not identified with much confidence. These vibrational type couplings are characteristic of weak coupling to a spherical Pb core. Ordinarily, proton particle states would not be expected, as they would lie high in energy above the shell gap, but it is seen that the $h_{9/2}$ and $i_{13/2}$ orbitals intrude below the gap to form shell-model states of protons strongly coupled to oblate Hg cores. It is possible that the $f_{7/2}$ proton state is observed here, too, but the levels in question have also been attributed to the $h_{9/2}$ structure.

The structure of levels built on the $h_{9/2}$ proton particle state shows excellent agreement with the structure predicted by calculations according to the triaxial-rotor-plus-particle model of Meyer-ter-Vehn. It appears that the ^{193}Tl nucleus is well modeled by a proton coupled

to a rigid triaxial shape. The Fermi surface did have to be raised substantially to produce levels that would account for an observed side band, but this could be accounted for by mixing between $h_{9/2}$ and $f_{7/2}$ orbitals. It is these levels that might actually be an $f_{7/2}$ single-particle structure.

The proposed structure built on deformed ^{192}Hg or ^{194}Pb cores and decaying by E0 transitions were not seen. The conversion electron data is good enough that they should have been in evidence unless they exist as a doublet or in a highly complicated portion of the spectrum.

LIST OF REFERENCES

LIST OF REFERENCES

1. R. M. Diamond and F.S. Stephens, Nuclear Physics 45, 632 (1963)

2. J. O. Newton, F. S. Stephens and R. M. Diamond, Nuclear Physics A236, 225 (1974)

3. J. H. Hamilton, K. R. Baker, C. R. Bingham, E. L. Bosworth, H. K. Carter, J. D. Cole, R. W. Fink, G. Garcia Bermudez, G. W. Gowdy, K. J. Hofstetter, M. A. Ijaz, A. C. Kahler, B. D. Kern, W. Lourens, B. Martin, R. L. Mlekodaj, A. V. Ramayya, L. L. Riedinger, W. D. Schmidt-Ott, E. H. Spejewski, B. N. Subba Rao, E. L. Robinson, K. S. Toth, F. Turner, J. L. Weil, J. L. Wood, A. Xenoulis and E. F. Zganjar, Izvestiya Akademii Nauk SSSR. Seriya Fizicheskaya, Vol. 40, No. 1, 2 (1976)

4. A. C. Kahler, Ph.D. Dissertation, The University of Tennessee, Knoxville, Tennessee, 1978

5. L. L. Collins, L. L. Riedinger, A. C. Kahler, J. L. Wood, R. W. Fink, A. G. Schmidt, E. H. Spejewski, H. K. Carter, R. L. Mlekodaj, E. F. Zganjar and J. H. Hamilton, to be published

6. J. A. Bounds, C. R. Bingham, P. Juncar, H. K. Carter, G. A. Leander, R. L. Mlekodaj, E. H. Spejewski and W. M. Fairbank, Jr., to be published

7. J. Meyer-ter-Vehn, Nuclear Physics A249, 111 (1975)

8. J. Meyer-ter-Vehn, Nuclear Physics A249, 141 (1975)

9. A. S. Davydov and G. F. Fillipov, Nuclear Physics 8, 237 (1958)

10. L. L. Riedinger, A. C. Kahler, L. L. Collins and G. D. O'Kelly, to be published

11. P. Van Duppen, E. Coenen, K. Deneffe, M. Huyse, K. Heyde and P. Van Isacker, Physical Review Letters Vol. 52, No. 22, 1974 (1984)

12. E. F. Zganjar, J. D. Cole, J. L. Wood, G. Gowdy and L. L. Riedinger, Bulletin of the American Physical Society, Series II, Vol. 29, No. 7, 1049 (1984)

13. The Radiochemical Centre; Amersham, England, Certificate for Source No. 0307QB

14. F. Rosel, H. M. Fries, K. Alder and H. C. Pauli, Atomic Data and Nuclear Data Tables, Vol. 21, No. 4, 293 (1978)

15. National Bureau of Standards, Certificate for Standard Reference Material SRM 4275-4

16. B. Amov, T. Vandlik, J. Vandlik, T. Vylov, Z. Zhelev, N. G. Zaitseva, I. Penev and H. Tyrroff, Soviet Journal of Nuclear Physics 16, 487 (1973)

17. M. Pautrat, G. Albouy, J. C. David, J. M. Lagrange, N. Poffe C. Roulet, H. Sergolle, J. Vanhorenbeeck and H. Abou-leila Nuclear Physics A201, 449 (1973)

18. L. L. Collins, Ph.D. Dissertation, The University of Tennessee, Knoxville, Tennessee, 1978

VITA

Grady Campbell was born in Clearwater, Florida on February 1, 1955. He graduated from Charles E. Jordan High School of Durham, North Carolina in June 1973. The following September he entered Emory University in Atlanta, Ga. and in June 1977 he received a Bachelor of Science degree, with a major in Physics. In August of that year he began employment at EG&G ORTEC in Oak Ridge, Tennessee. In the fall of 1979 he enrolled as a part-time student at the University of Tennessee, Knoxville and began study toward a Master's degree, with a major in Physics. This degree was awarded in August 1985.